Atomic resolution nanomechanical mass sensor

FEM Modeling Report
Fall 2024

Mehdi Amor
Shristi Shrivastava
Tirui Wang

Professor: Andras Kis

March 26, 2025

Contents

1 Introduction **3**

2 Theory **3**

3 Methodology and Simulation **4**

3.1 General Concept 4

3.2 Materials and Physics Modules 6

4 Results and Discussion **6**

4.1 Input voltage and Deflection 6

4.2 Maximum Distance between Electrodes for Field Emission 8

4.3 Resonance Frequency Shift 10

5 Annexes **12**

1 Introduction

This project focuses on a NEMS device that can achieve atomic resolution mass detection at room temperature. The device comprises of a carbon nanotube (CNT) fixed to an electrode at one end and free to oscillate at the other end. A counter-electrode is placed opposite the nanotube enabling oscillations through the application of an alternating voltage at a frequency equal to the nanotube's resonant frequency. At high electric fields (E > 1 V/µm), field emission occurs at the nanotube's tip. There is a strong coupling between the field emission current and the nanotube's mechanical vibrations. Hence this measurable current can be used to detect the nanotube's motion.

An important feature of this device is the use of singly clamped geometry. There are many advantages of a singly clamped geometry over the commonly used doubly clamped ones. They have a larger dynamic range and higher quality factor due to reduced clamping losses. These properties are specially useful for achieving high sensitivity in mass detection. Additionally, double-walled nanotubes provide greater rigidity and uniform electrical properties compared to single-walled nanotubes, which enhances the device's performance and reliability.

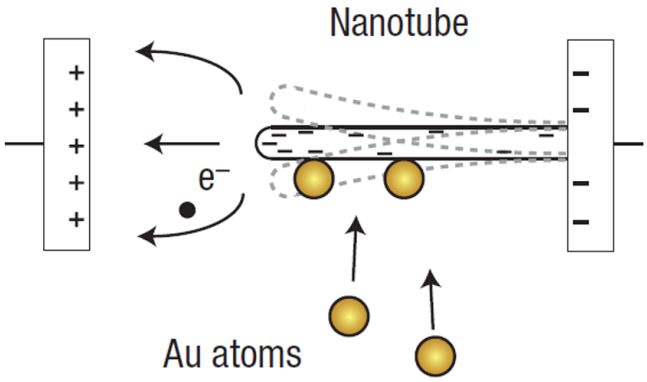

Figure 1: Nanotube detector based on field emission

Another notable effect happening in this arrangement is the field enhancement effect. It is a phenomenon where due to the way the electric field interacts with the geometry of the material, the electric field becomes much stronger at sharp or small structures as compared to the surrounding areas. Hence, more electric field lines are concentrated at the tip of the carbon nanotube.

2 Theory

When a voltage is applied between the two electrodes, the cantilever and the counter electrode form a capacitor. This leads to a separation of charges and the creation of an electric field between them. Due to the geometry, the electric field is not uniform. Instead, it becomes stronger in certain regions, typically towards the tip of the cantilever, where the charges get compacted and the electric field is locally radial. Due to the asymmetry of the beam in the y-axis (from the fabrication process), the force applied on each part of the beam is not equal which will generate a bending of the beam in the perpendicular direction, following the equation $\mathbf{F} = q\mathbf{E}$.

When an AC voltage is applied, the capacitor repeatedly charges and discharges, inducing oscillations in the cantilever. The system has a characteristic natural frequency [1]:

$$\omega_0 = \sqrt{\frac{k_{\text{eff}}}{m_{\text{eff}}}} \approx \sqrt{\frac{3 \cdot YI/L^3}{0.24 \cdot \rho AL}} \tag{1}$$

with Y being the Young's modulus, I the areal moment of inertia, ρ the density, A the cross-sectional area and L the length of the beam.

By deriving 1, we get :

$$\left|\frac{dm}{m}\right| = 2\frac{d\omega}{\omega} \tag{2}$$

From this equation, we can conclude that for a lighter beam, the sensitivity of the system is higher.

If the applied AC frequency matches this natural frequency, resonance occurs, making the cantilever oscillate with significantly greater amplitude. The purpose of this device is to monitor changes in the resonance frequency of the cantilever beam caused by nanoscale masses attaching to it. These changes in resonance frequency can then be used to accurately determine the value of the attached masses, as described by the equation 3, [1]:

$$\Delta f = \overline{R(x)} \cdot \Delta m = -\frac{f_0}{2m_0}\Delta m \tag{3}$$

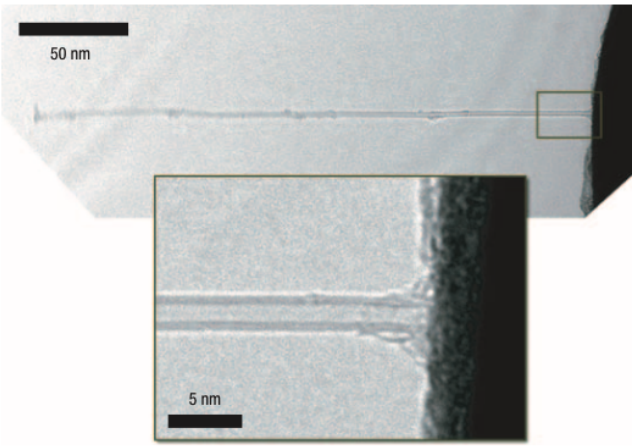

Figure 2: TEM images of a nanomechanical mass spectrometer device constructed from a double-walled carbon nanotube [1]

3 Methodology and Simulation

3.1 General Concept

Two COMSOL models are used for the simulation. The first model is a 2D planar setup, comprising two rectangular electrodes measuring 5 nm x 30 nm, with a cylindrical tube of

225 nm length (Figure 2) and 1.4 nm diameter attached to one of them. The beam is placed 0.5 nm off-center relative to the electrode to introduce an asymmetry. The entire system is enclosed within a large circular domain of 20 um diameter, representing the dielectric material. It is designed to be sufficiently large to enable movement of the electrodes without significant interference between the dielectric boundaries and the electric field generated by the charges.

The second model is based on 2D axisymmetry setup (Figure 5). It represents a 3D model constructed by rotating the 2D sketch with respect to the axis of symmetry, thus the computation is largely simplified compared to a regular 3D model. The nanotube in this setting is perfectly cylindrical, and the electrodes are abstracted as two parallel planes without thickness, which serve as ideal circuitry boundaries. Basically the same set of parameters are used across the two models as summarized in COMSOL (see Figure 6).

Figure 3: Square-shaped nanotube edge for a diameter of 1.5nm

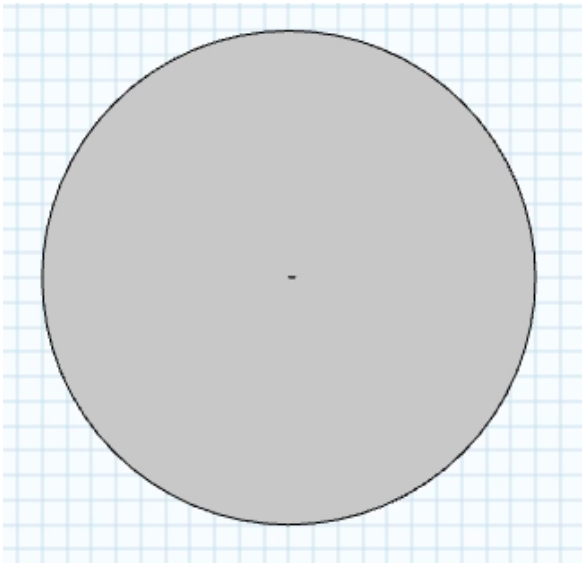

Figure 4: Circle-shaped nanotube edge for a diameter of 1.6nm

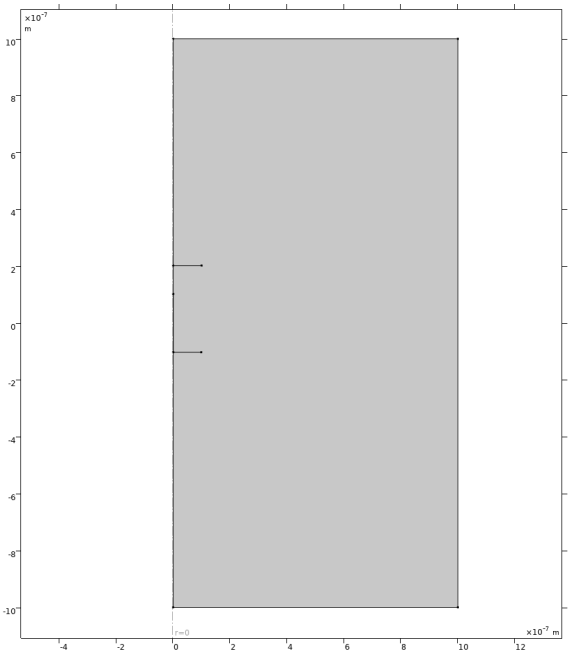

Figure 5: 2D axisymmetry model representation

Name	Expression	Value	Description
V_dc	100 [V]	100 V	
L_CNT	205 [nm]	2.05E-7 m	
Do_CNT	1.78 [nm]	1.78E-9 m	
Di_CNT	1.44 [nm]	1.44E-9 m	
m_CNT	1.58e-21 [g]	1.58E-24 kg	
D_CNT	1.4 [nm]	1.4E-9 m	
E_CNT	1 [TPa]	1E12 Pa	Young`s modulus
y_CNT	0.27	0.27	Poisson ratio
d	100 [nm]	1E-7 m	gap distance
density_C...	m_CNT/(L_CNT*(Do_CNT^2)/4*pi)	3.0972 kg/m³	

Figure 6: Parameters defined in COMSOL

3.2 Materials and Physics Modules

For the electrodes, aluminum was selected for its high electrical conductivity and compatibility with nanofabrication techniques, making it well-suited for this application. The beam is composed of a custom carbon nanotube material, as the Young's modulus and Poisson's ratio and density are customized; the properties are summarized in Figure 7. The surrounding dielectric medium is vacuum.

	Property	Variable	Value	Unit	Property group
☑	Relative permittivity	epsilonr_iso...	1	1	Basic
☑	Density	rho	3	kg/m³	Basic
☑	Young's modulus	E	1[TPa]	Pa	Young's modulus and Poisson's ratio
☑	Poisson's ratio	nu	0.27	1	Young's modulus and Poisson's ratio
	Electrical conductivity	sigma_iso ;...	35.5e6[S/m]	S/m	Basic

Figure 7: Material Properties of carbon nanotube

Three packages were used in this project: the Electrostatics module to create the potential difference and calculate the electrostatic force on the beam, the Solid Mechanics module to simulate the beam's bending in response to the applied force, and the Moving Mesh module to ensure the mesh dynamically adapts to the beam's deformation. These implementations are detailed in the project file. To simulate the oscillating state, eigenfrequency study is performed after soloving the static state of the electric field.

4 Results and Discussion

4.1 Input voltage and Deflection

The electrostatic force induced deflection on the nanotube cantilever is related to the voltage applied across the electrodes. To our knowledge, the total force results in a pulling effect on the longitutional direction of the nanotube, creating tension in the material. (Demonstrated by simulation in 8) If the nanotube is not symmetrical across the cross-section, which is usually the case from the fabrication, the electric field will result in a net lateral force for the nanotube to deflect.

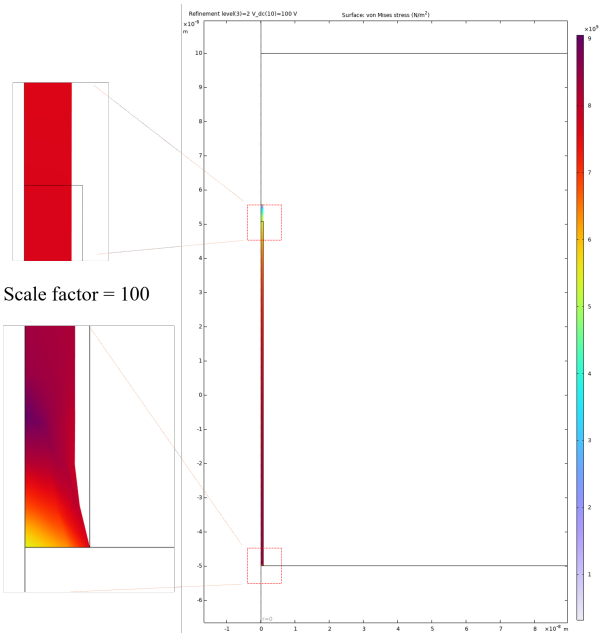

Figure 8: Presentation of the nanotube elongation

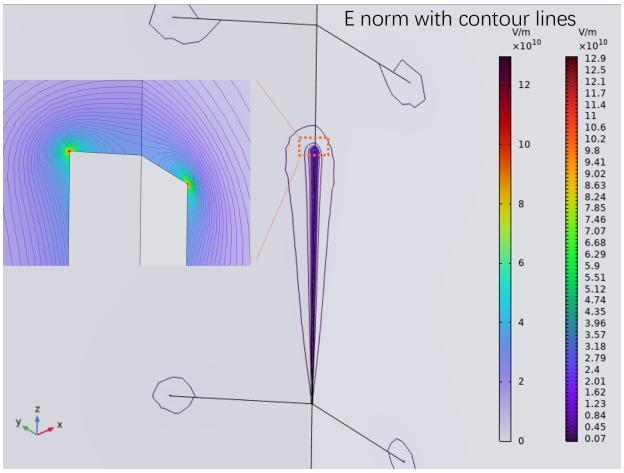

Figure 9: Electric field norms across the structure

The relative displacement is ploted in (Figure 10). The deformation can reach 0.8% under the maximum static applied DC offset, 100V in our case. It's roughly in the trend of a parabolic shape, which corresponds to the displacement is proportional to V_{dc}^2. For a linear elastic material, the displacement is proportional to the force applied and the electrostatic force is proportional to V_{dc}^2.

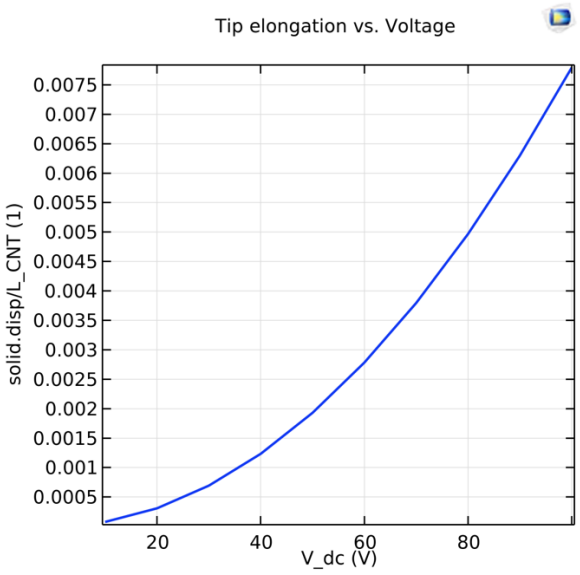

Figure 10: Nanotube deformation with voltage

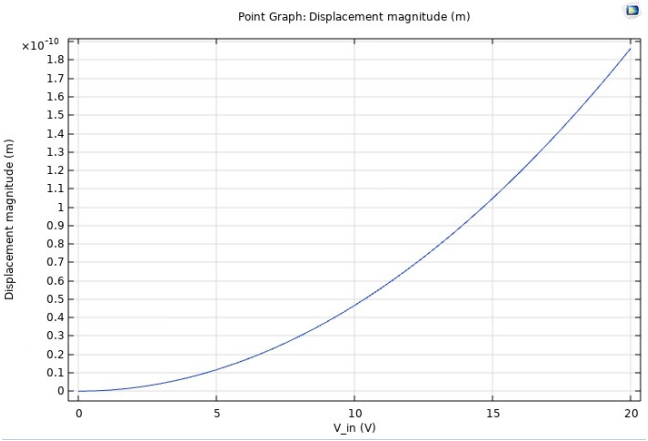

Figure 11: Voltage applied between the two electrodes vs the deflection of the nanotube in the middle

The graph of the voltage applied between the electrodes vs the deflection of the nanotube here (Figure 11) increases in a roughly parabolic trend as explained above.

The condition that should be satisfied in order to get a deflection to occur - first, the electric field at the nanotube's tip should be high enough, (greater than 1V/µm). Also, the asymmetric geometry of the nanotube ensures that the forces do not cancel out, which allows the deflection to take place.

4.2 Maximum Distance between Electrodes for Field Emission

When computing the maximum distance between the counter-electrode and the tip of the beam, the electric field norm at the tip consistently exceeded the threshold of 10^6 V/m required for field emission, even at significantly larger distances than anticipated, due to the field enhancement. For instance, at a distance of 700 μm, the electric field at the tip reached 2.02×10^8 V/m (see Annex 18).

Increasing the distance further led to issues with the simulation setup, as making the dielectric circle significantly larger than the electrodes and beam resulted in deformations of the electrodes geometry (radius = 2 mm and above, see Annex 19), or in a non convergence of the solver. To overcome these limitations, performing an input voltage sweep (0.05V, 0.5, 100V) was chosen to determine the input voltage required for the emission field to be generated, using this data to calculate the distance.

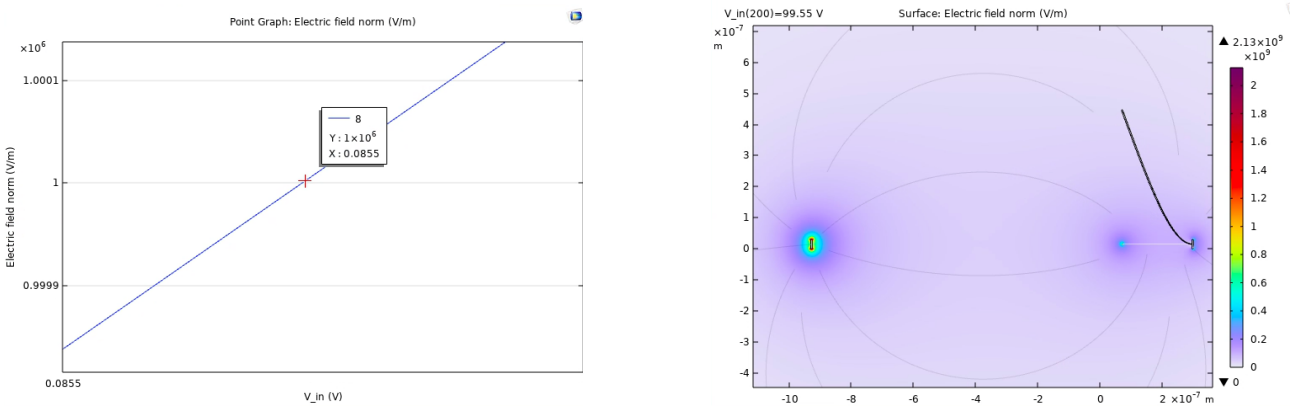

(a) (b)

Figure 12: Field emission threshold and electric field distribution for a nanotube-counter electrode distance of $d = 1000\,\text{nm}$.

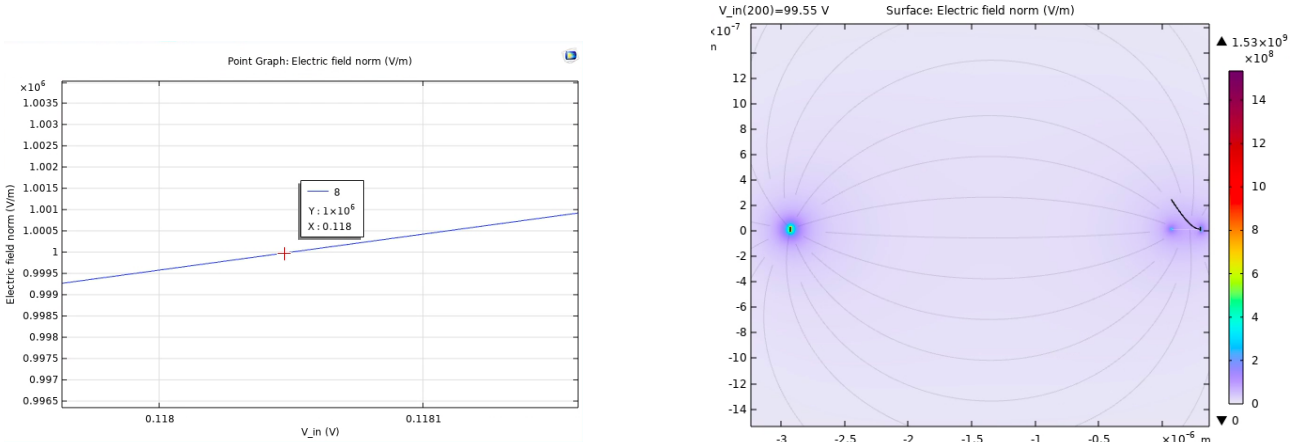

(a) (b)

Figure 13: Field emission threshold and electric field distribution for a nanotube-counter electrode distance of $d = 3000\,\text{nm}$.

We can calculate the electric field at the tip as the uniform one multiplied by a enhancement field coefficient β that takes into consideration the concentration of the electric field [2] :

$$E_{\text{local}} = \beta \cdot E \quad \text{with} \quad E = \frac{V}{d}$$

The equivalent input voltage required to generate an electric field of $10^6\,\text{V/m}$ is $0.085\,\text{V}$ for $d = 1000\,\text{nm}$ (see Figure 12a), and $0.118\,\text{V}$ for $d = 3000\,\text{nm}$ (see Figure 13a). Using these values, the field enhancement factor β can be computed to determine its value for an input voltage of $100\,\text{V}$.

Distance (nm)	**Reference Field ($E = V/d$, V/m)**	**Local Field (E_{local}, V/m)**	$\beta = \frac{E_{\text{local}}}{E}$
500	1.39×10^5	1.0×10^6	7.2
1000	8.55×10^4	1.0×10^6	11.7
7000	3.68×10^4	1.0×10^6	27.17
100 000	1018	1.0×10^6	1018
400 000	283	1.0×10^6	3533
700 000	185	1.0×10^6	5393

Table 1: Comparison of macroscopic field, local field, and field enhancement factor β for different distances.

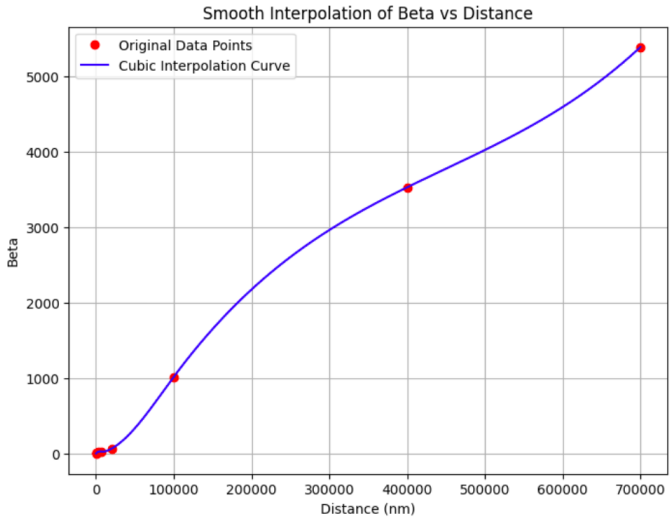

Figure 14: Interpolation of the relation between β and d from discrete datapoints 20

It can be observed that β exhibits an approximate linear dependence on the distance between the counter-electrode and the tip. Specifically, β decreases as the distance decreases. This behavior can be explained by the fact that, at shorter distances, the influence of the radially concentrated electric field diminishes relative to the direct horizontal component of the field. In all cases though, the overall electric field strength increases as the distance decreases.

We get $\beta(d) \approx 30 + 0.08 \cdot d$, and for $V_{\text{in}} = 100\,\text{V}$ and $E = 10^6\,\text{V/m}$:

$$d = \beta(d) \cdot \frac{V}{E_{\text{local}}} \quad \approx 3\,\text{mm}$$

4.3 Resonance Frequency Shift

To compute the resonant frequency in COMSOL, Eigenfrequency study was employed based on the deformation from static calculation. By calculating the theoretical resonant frequency from the equation 1 based on the geometry parameters, the target of the resonant frequency is set to be 300 MHz. In COMSOL, the first eigenfrequency is used to converted to resonant frequency in the relation of $\omega_i = 2\pi \cdot f_i$. The settings windows in COMSOL is shown in figure 15:

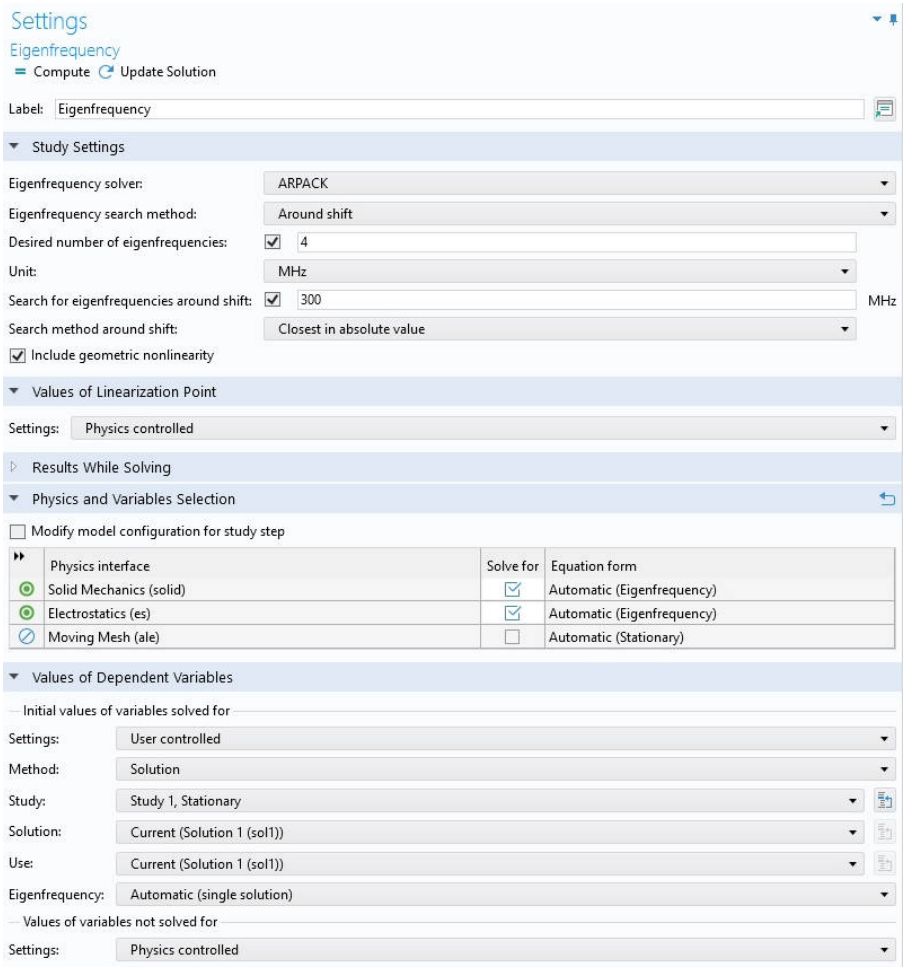

Figure 15: COMSOL windows for eigenfrequency study

In theory, the voltage applied on the opposite electrode will attract the carbon nanotube therefore increasing the spring constant k_{eff}. The results from COMSOL comply with the predicted trend that the resonant frequency goes up with the increasing voltage difference across the electrodes. As shown in the following graph 16, the change from 10V to 100V under out settings leads to a varience of roughly 5 MHz in the resonant frequency.

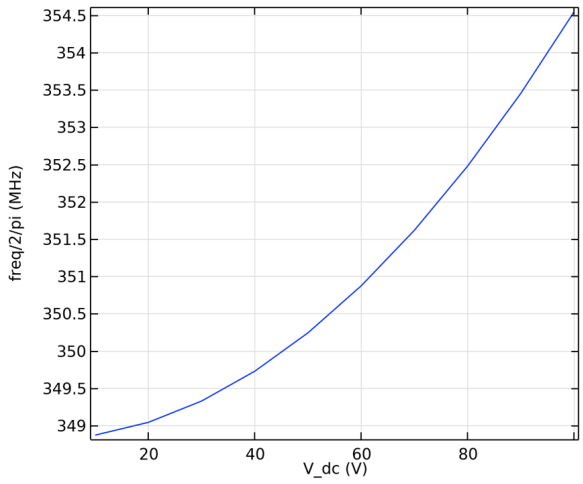

Figure 16: Resonant frequency plot with voltage applied

5 Annexes

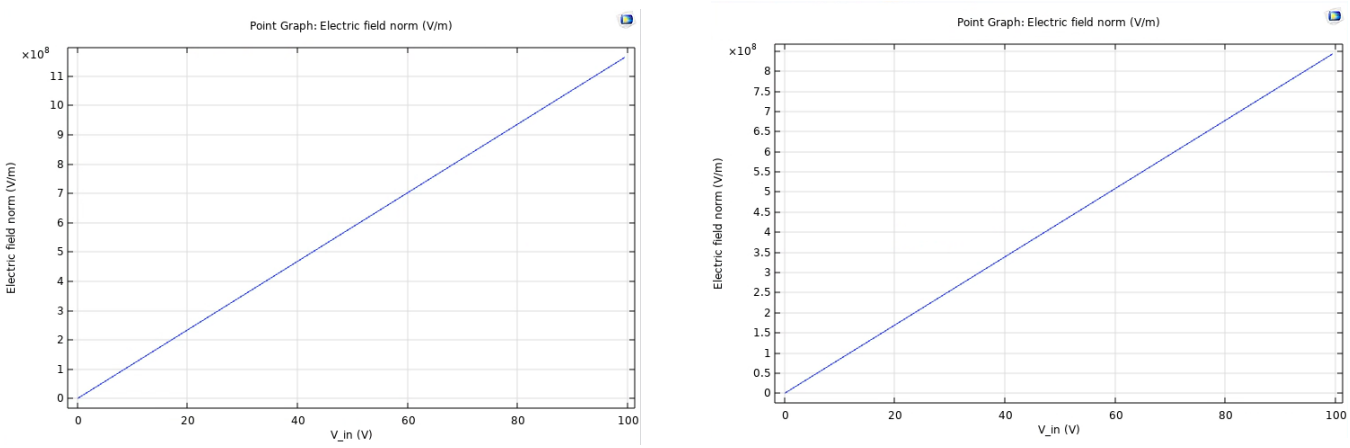

(a) (b)

Figure 17: Electric field norm comparison at different distances: (a) $d = 1000\,\text{nm}$, (b) $d = 3000\,\text{nm}$.

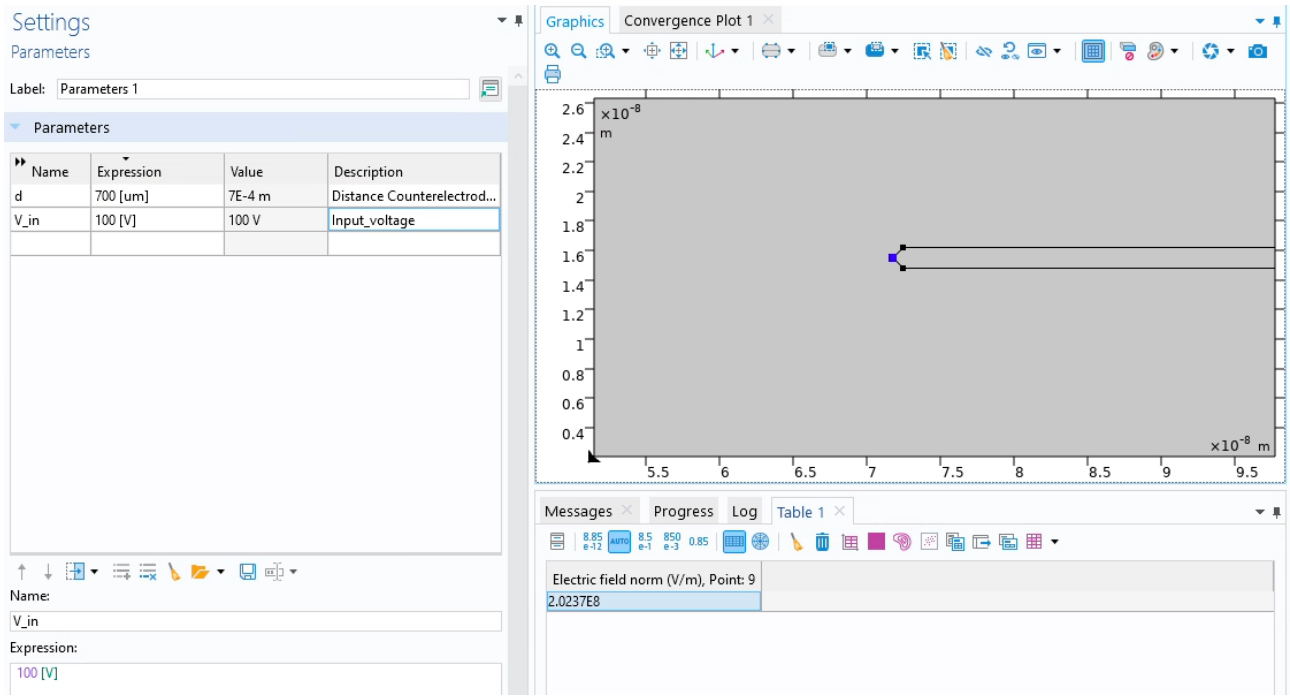

Figure 18: Electric field norm at the tip data for d = 700um and Vin = 100V

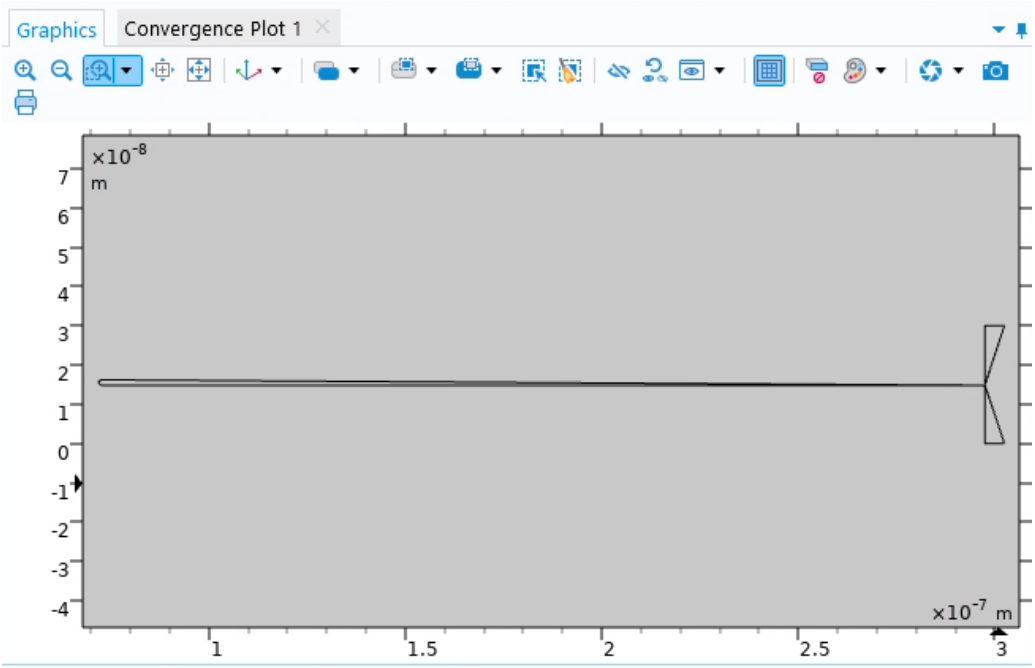

Figure 19: Deformation of the electrode and beam geometry observed when the dielectric domain is excessively large.

```python
import numpy as np
import matplotlib.pyplot as plt
from scipy.interpolate import interp1d

# Data points
# Distances in nm
d_values = np.array([200, 500, 1000, 3000, 7000, 20000, 100000, 400000, 700000])
beta_values = np.array([2.26, 7.2, 11.7, 25.6, 27.17, 65.35, 1018, 3533, 5393])

# Create an interpolation function
interp_function = interp1d(d_values, beta_values, kind='cubic')

# Generate a smooth range of distances for interpolation
d_smooth = np.linspace(min(d_values), max(d_values), 500)
# 500 points between 200 and 7000
beta_smooth = interp_function(d_smooth)
```

Figure 20: Python code for interpolating `beta` values using cubic splines

References

[1] K. Jensen, K. Kim, and A. Zettl, "An atomic-resolution nanomechanical mass sensor," *Nature Nanotechnology*, vol. 3, no. 9, p. 533–537, Jul. 2008. [Online]. Available: https://www.nature.com/articles/nnano.2008.200#citeas

[2] F. Giubileo, A. Di Bartolomeo, L. Iemmo, G. Luongo, and F. Urban, "Field emission from carbon nanostructures," *Applied Sciences*, vol. 8, no. 4, 2018. [Online]. Available: https://www.mdpi.com/2076-3417/8/4/526